Landslides (2016) 13:399–410
DOI 10.1007/s10346-015-0663-5
Received: 21 April 2015
Accepted: 23 November 2015
Published online: 5 December 2015

Andrea Ciampalini · Federico Raspini · William Frodella · Federica Bardi · Silvia Bianchini · Sandro Moretti

The effectiveness of high-resolution LiDAR data combined with PSInSAR data in landslide study

Abstract The spatial resolution of digital elevation models (DEMs) is an important factor for reliable landslide studies. Multi-interferometric techniques such as persistent scatterer interferometric synthetic aperture radar (PSInSAR) are used to evaluate the landslide state of activity and its ground deformation velocity, which is commonly measured along the satellite line of sight (LOS). In order to compare velocities measured by different satellites in different periods, their values can be projected along the steepest slope direction, which is the most probable direction of real movement. In order to achieve this result, DEM-derived products are needed. In this paper, the effectiveness of different DEM resolutions was evaluated in order to project ground deformation velocities measured by means of PSInSAR technique in two different case studies in the Messina Province (Sicily, southern Italy): San Fratello and Giampilieri. Three DEMs were used: (i) a 20-m resolution DEM of the Italian Military Geographic Institute (IGM), (ii) a 2-m resolution DEM derived from airborne laser scanning (ALS) light detection and ranging (LiDAR) data for the San Fratello 2010 landslide, and (iii) a 1-m resolution DEM derived from ALS LiDAR data for the area of Giampilieri. The evaluation of the applied method effectiveness was performed by comparing the DEMs elevation with those of each single permanent scatterer (PS) and projecting the measured velocities along the steepest slope direction. Results highlight that the higher DEM resolution is more suitable for this type of analysis; in particular, the PS located nearby the watershed divides is affected by geometrical problems when their velocities are projected along the steepest slope.

Keywords Landslide · PSInSAR · DEM · Velocity projection · LiDAR

Introduction

Spaceborne synthetic aperture radar (SAR) images are currently used to detect, monitor, and forecast active geological processes leading to ground deformation. For example, SAR data have been extensively used to study subsidence phenomena (Tomás et al. 2005; Raspini et al. 2012; Rosi et al. 2014). tectonic (Massironi et al. 2009; Vilardo et al. 2009; Lagios et al. 2013). earthquakes (Lagios et al. 2012; Luo et al. 2013). and volcanic activity (Peltier et al. 2010). Among ground deformation phenomena, landslides represent one of the most studied natural hazards by using this technique (Herrera et al. 2009; Notti et al. 2010; Meisina et al. 2013; Tofani et al. 2013; Oliveira et al. 2014). Differential synthetic aperture radar (DInSAR) represents the basic technique which exploits the phase difference between two SAR images acquired in different periods producing interferograms (Gabriel et al. 1989). More recently, several different multi-interferometric techniques have been developed, such as persistent scatterer interferometric synthetic aperture radar (PSInSAR) (Ferretti et al. 2001) and SqueeSAR (Ferretti et al. 2011). Small Baseline Subset (Berardino et al. 2002). Stable Point Network (Arnaud et al. 2003) and Coherent Pixel Technique (Mora et al. 2003). These techniques use an extensive archive of satellite radar data (dating back to 1992) in order to identify networks of persistently scattering (i.e., radar reflecting) features, such as buildings and bridges, or natural features, such as rocky outcrops, against which relatively precise motion measurements are calculated retrospectively over the time spanned by the data archive. Landslide mapping and monitoring can greatly benefit from spaceborne InSAR data analysis because of its great cost-benefit ratio (especially by using archival data), non-invasiveness, wide area coverage, and high precision (Crosetto et al. 2010; Frattini et al. 2013; Wasowski and Bovenga 2014). Spaceborne multi-interferometric SAR techniques measure ground motion, with millimeter accuracy, representing a useful tool to detect and characterize slow surface phenomena, rapidly providing products such as landslide inventory and state of activity maps (Bovenga et al. 2006; Colesanti and Wasowski 2006; Cascini et al. 2009; Hung et al. 2011; Ciampalini et al. 2012; Raspini et al. 2012; Bianchini et al. 2013; Del Ventisette et al. 2013; Bianchini et al. 2014).

Several studies have investigated the role of the digital elevation model (DEM) spatial resolution and its impact on landslide investigations (Glenn et al. 2006; Kasai et al. 2009; Keijesers et al. 2011; Jabayedoff et al. 2012; Tarolli 2014) by comparing results obtained through the use of both low and high spatial resolution DEMs. During the last years, the increase in the use of very high-resolution DEM derived by light detection and ranging (LiDAR) data led to an improvement in terrain analysis, highlighting the advantages and limitations with respect to the low-resolution DEM (Classens et al. 2005; Ardizzone et al. 2007; Chen et al. 2013; Fuchs et al. 2014; Tarolli 2014). For example, LiDAR-derived DEM has been extensively used in landslide studies (Jabayedoff et al. 2012 and reference therein). for the characterization of channel networks (Montgomery and Foufoula-Georgiu 1993; Tarolli and Dalla Fontana 2009; Cavalli et al. 2008), for river morphology analysis (Jones et al. 2007; Marcus and Fonstad 2010). active tectonic deformation recognition (Cunningham et al. 2006; Oskin et al. 2007). and in the detection of morphological changes in volcanic environments (Davila et al. 2007; Csatho et al. 2008). Considering the abovementioned works, the effectiveness of high- or low-resolution DEM in landslide study depends on the purpose of the research. On the other hand, several studies on landslide susceptibility assessment highlighted that low- to medium-resolution DEM can be more suitable (Catani et al. 2013). Normally, the optimal resolution of a DEM is directly related to the average size of the investigated hillslope process (Tarolli 2014) and also to the target of the investigation (hazard assessment, geotechnical study, risk evaluation, etc.). PSInSAR post processing analysis can benefit from its combination with DEM data for a more accurate evaluation of the landslide kinematic. For each detected permanent scatterer (PS), both displacements and ground deformation velocity are measured by the satellite sensor

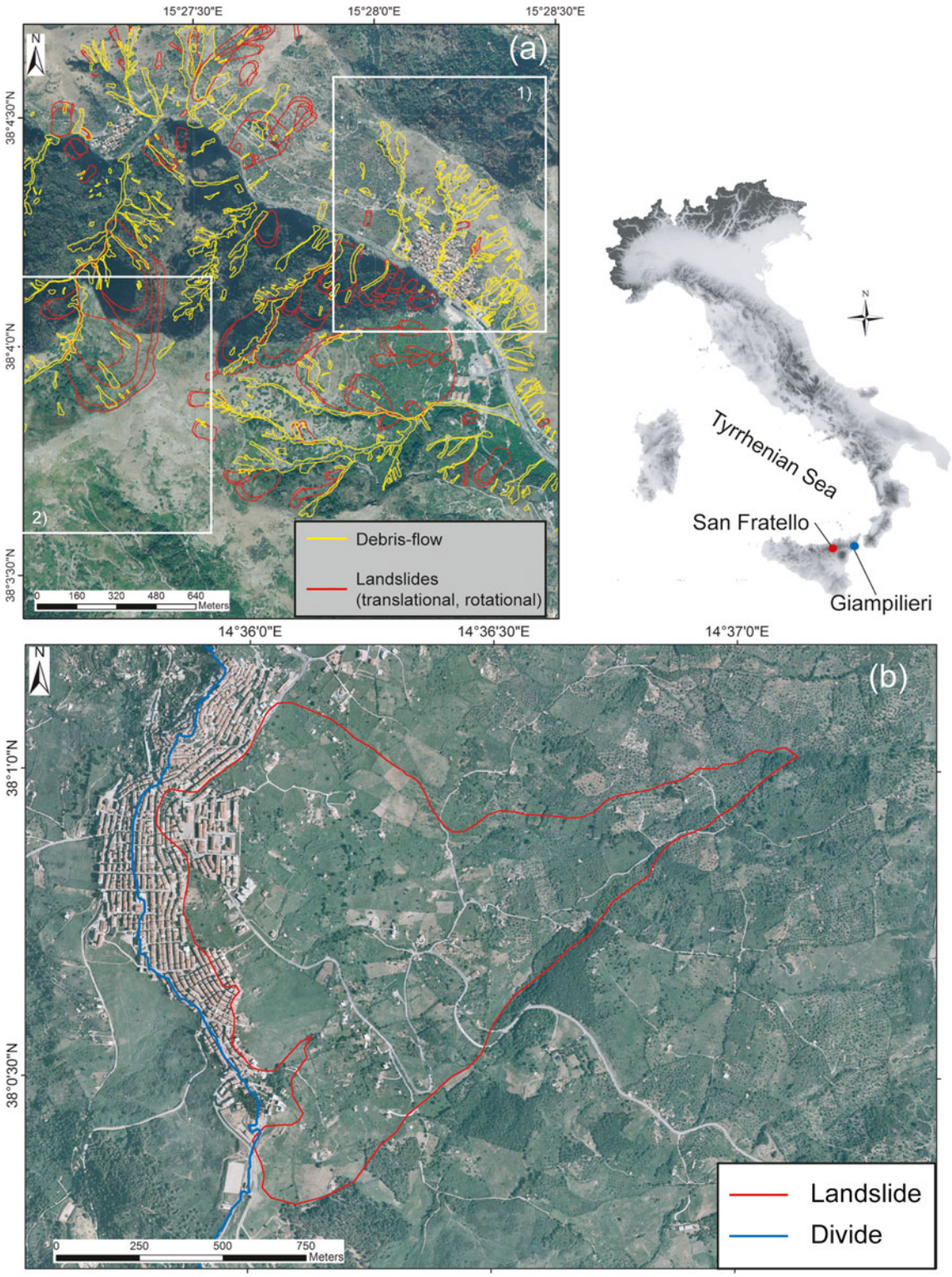

Fig. 1 Location of the study areas: **a** Giampilieri and **b** San Fratello. The landslide inventory map in **a** is from Ardizzone et al. 2012. The landslide boundary in **b** is from Bardi et al. 2014. *White rectangles* (*1* and *2*) in **a** correspond to the area showed in Fig. 9

along its line of sight (LOS) even though the real displacement, which results slightly underestimated, actually occurs in three dimensions (Cascini et al. 2009). PSInSAR velocities in landslide studies are commonly used in the component measured along the LOS (Cigna et al. 2012; Meisina et al. 2008; Oliveira et al. 2014; Uzielli et al. 2015). A more reliable velocity measure can be obtained by projecting the velocity measured in the LOS direction, along the steepest slope considered as the most probable real movement direction (Notti et al. 2014; Bianchini et al. 2014). The velocity projection along the steepest slope uses the products

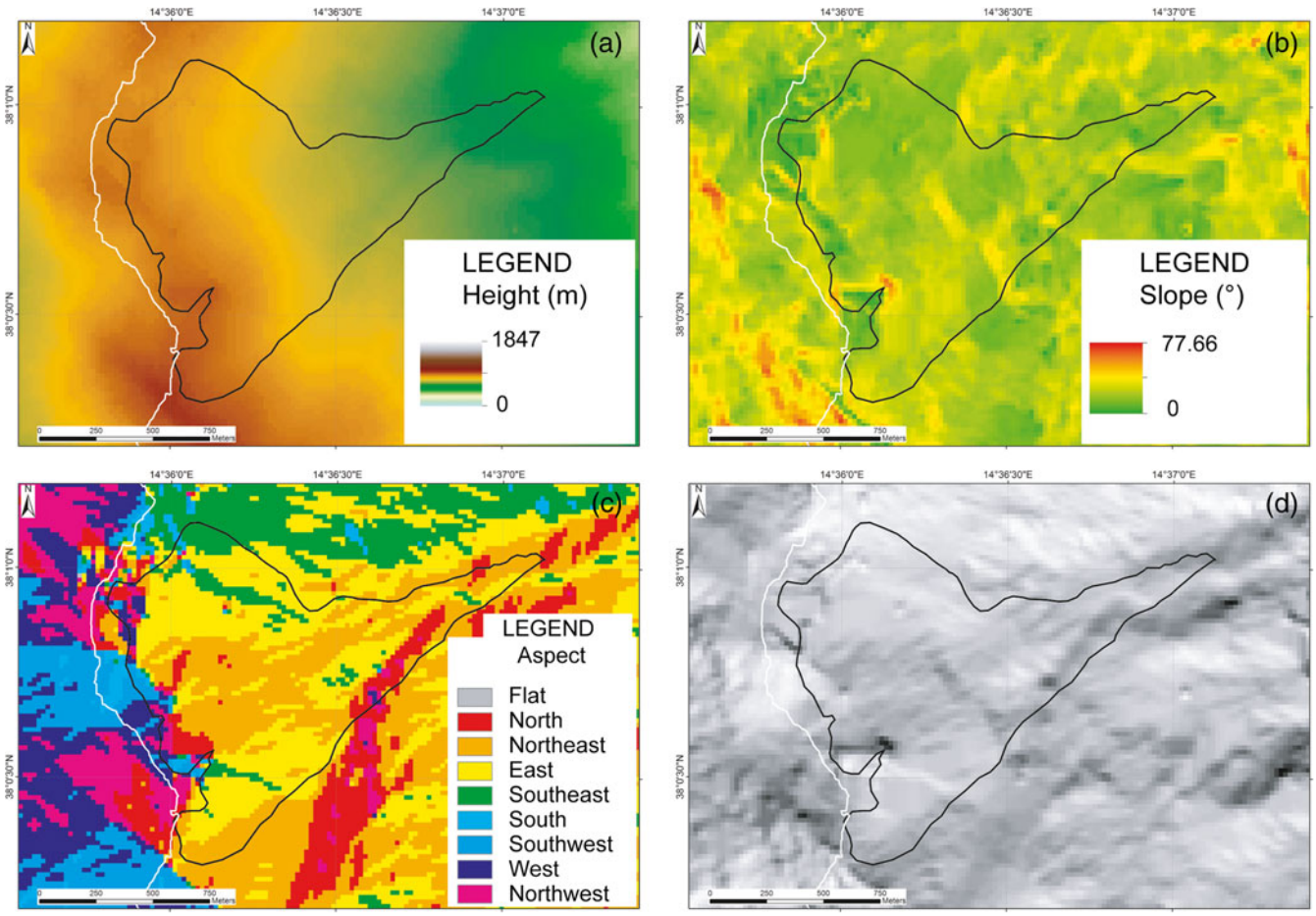

Fig. 2 Example of the 20-m resolution DEM-derived products for the area of San Fratello. **a** DEM, **b** slope, **c** aspect, and **d** hillshade. The *white line* is the watershed divide; the *black line* corresponds to the 2010 landslide boundary

derived from a DEM of the analyzed area, besides the satellite acquisition parameters (azimuth, incidence angle, and directional cosines) of the LOS. In order to achieve this result, a low- to medium-resolution DEM or a resample of a detailed DEM is recommended (Notti et al. 2014) with the aim of reducing the effect of terrain roughness and the presence of counterslopes. This work evaluates the usefulness of DEMs characterized by different spatial resolutions, during the multi-temporal analysis of PSInSAR post processing phase, in order to improve the effectiveness of this type of data in landslide kinematic analysis. The DEM resolution evaluation was tested in the Messina Province (Sicily, Italy), an area strongly affected by landslide phenomena.

Study areas

The Messina Province (Sicily, Italy) is an area prone to landslides, due to the combination of different triggering (seismicity, exceptional rainfall events, active tectonics, and volcanic activity) and predisposing factors (lithology, land use, morphology) (Billi et al. 2008; Ciampalini et al. 2015). Between 2009 fall and 2010 winter on both the Nebrodi and Peloritani mountain ranges, exceptional rainfall events led to more than a thousand different types of mass movements: debris flows, complex, rotational, and translational landslides, rock falls (following the classification of Varnes 1978). which caused 37 victims, and intense damages to urbanized areas, infrastructures, and cultivated and pasture lands.

The San Fratello site

The first chosen area is San Fratello (Fig. 1), located along the Messina Province Tyrrhenian coastline, a town historically affected by landslide phenomena (Bardi et al. 2014; Ciampalini et al. 2014). It is located at an altitude of 675 m asl. The town is crossed by an important local roadway (SS 289) which connects several villages scattered within the Nebrodi mountains to the coastal highway. The inhabited area is located along the north–south-oriented divide between two watersheds, the Furiano Creek valley to the west and the Inganno Creek valley to the east. The eastern slope altitude varies between 250 m and 675 m asl. From the Inganno Creek valley up to the divide, the slope has gently rises from 250 to 620 m asl, with an average slope of 14°. From 620 m asl to the top of the divide, the average slope increase to 24° (Figs. 2 and 3). This morphology is probably linked to the presence of older landslides which modeled the slope. The most recent landslide event occurred on 14 February 2010, affecting a large sector of the eastern hillside, damaging several buildings and infrastructures (Bianchini et al. 2014). This landslide, about 1.8 km in length, involved an area of about 1 km^2, spanning from the town area eastern sector toward the Inganno Creek valley. This complex landslide produced also multiple failures, traction cracks, and counterslopes. In particular, the landslide is characterized by a rotational movement in its upper sector, evolving in an earth flow in its lower portion. From a geological point of view, the area of San Fratello is part of the northeastern sector of the

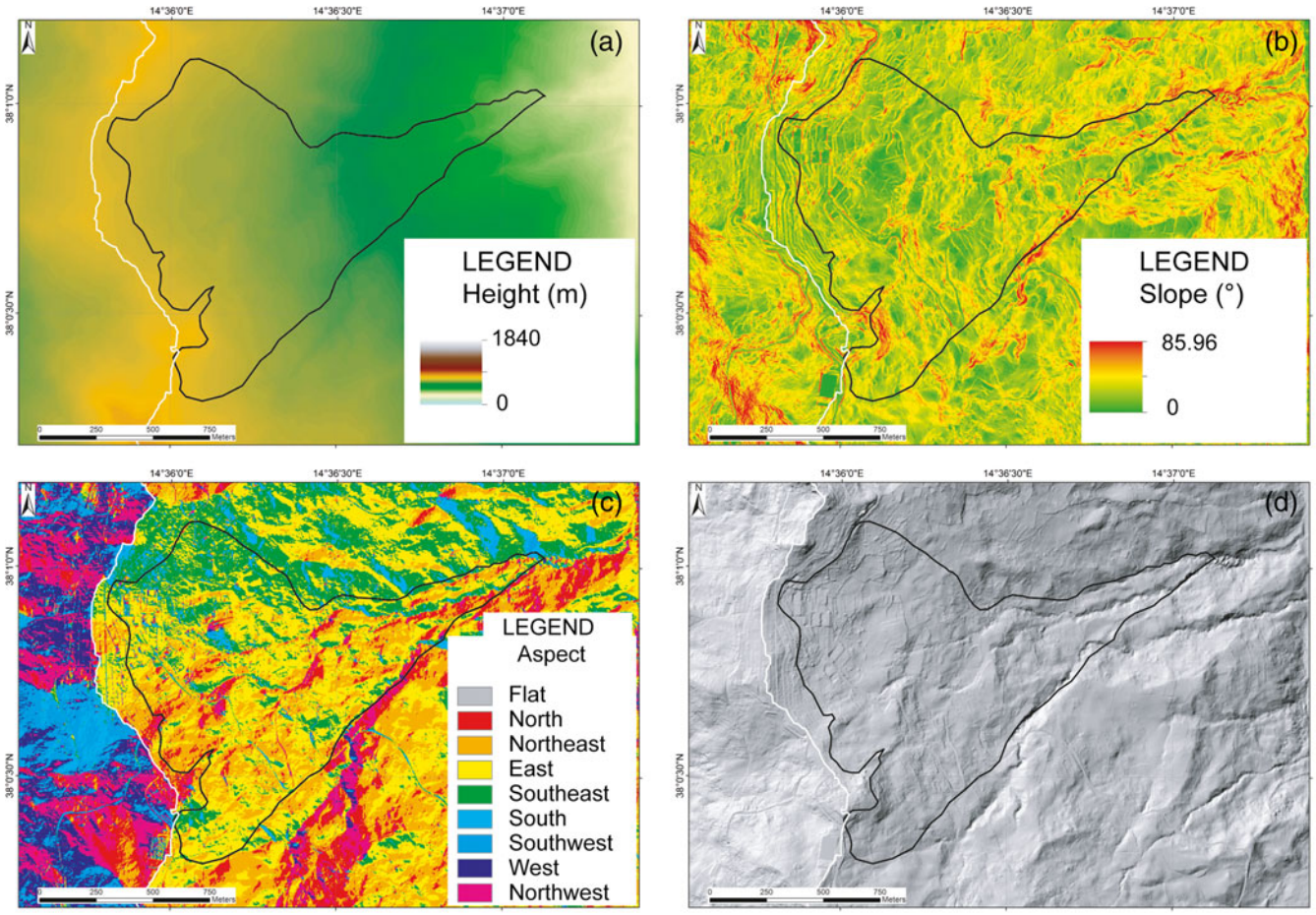

Fig. 3 Example of the 2-m resolution DEM derived products for the area of San Fratello. **a** DEM, **b** slope, **c** aspect, and **d** hillshade. The *white line* is the watershed divide; the *black line* corresponds to the 2010 landslide boundary

Apennine–Maghrebian orogenic belt. In particular, the area is characterized by the presence of a sequence of terrigenous to calcareous sedimentary sequences. The southern part of the village is made of terrigenous terrains, lower Cretaceous in age clayey sequences (Argille Scagliose unit). In the northern portion of the village, carbonate complexes, represented by Liassic limestone platform sequences crop out, overlapped by a terrigenous Late Eocene–Oligocene Flysch (Frazzano` Flysch). The top of the sequence is represented by the Cretaceous pelagic dolostones and limestones (San Marco D'Alunzio unit), which crops out in the N–NW San Fratello village area (Nigro and Sulli 1995; Lavecchia et al. 2007). The landscape of the study area and its slope instability are strongly influenced by this geological framework because of the overlapping of hard brittle lithologies on the soft clayey formations. Furthermore, the San Fratello area is characterized by a 10-m-thick cover of silty clayey sediments which increases the formation of slope instability phenomena.

The Giampilieri site

The second chosen study area is Giampilieri, located between the Messina Province Ionian coast and the Peloritani mountain ridge (Ardizzone et al. 2012; Del Ventisette et al. 2012) (Fig. 1), which on 1 October 2009, was hit by an exceptional storm (225 mm of rainfall recorded in 8 h). Giampilieri is located within the Giampilieri Creek valley on a southwest-oriented slope, which reaches its maximum altitude (516 m) about 2 km at northeast with respect to the village (Fig. 4). The urban area is developed between 128 and 190 m asl, and it is connected with the coastal highway by a single roadway axis, climbing upward along very steep slopes. In correspondence to the village, the slope rises up to 175 m asl, with an average angle of 10.5°. The slope increases rapidly until 180 m asl, with an average angle of 28° rising up to 44° between 180 m and 270 m asl. The highest part of the slope is characterized by a decrease of the angle (32°) (Fig. 4). The persisting rainfall triggered more than 600 slope failures, mainly shallow soil slides, debris flows, and debris avalanches, on an area of about 50 km^2. Giampilieri (Fig. 1) was the most damaged village, where landslides and floods caused 37 fatalities (including 31 deaths and 6 missing persons), 122 injured people and 2019 evacuated people (Ciampalini et al. 2015). The geological framework of the Giampilieri area is characterized by the presence of strongly weathered metamorphic rocks, topped by 1.5–2-m-thick weathered soil. The area northwestern sector is made of low-grade phyllites and metasandstones, whereas the southeastern sector of the village is made of medium-grade amphibolites of the Aspromonte unit (Del Ventisette et al. 2012). The contact between the amphibolites and the phyllites is represented by a fault. Both the lithologies appear deeply fractured and characterized by a cleavage system which reduces the geotechnical characteristic of the rocks.

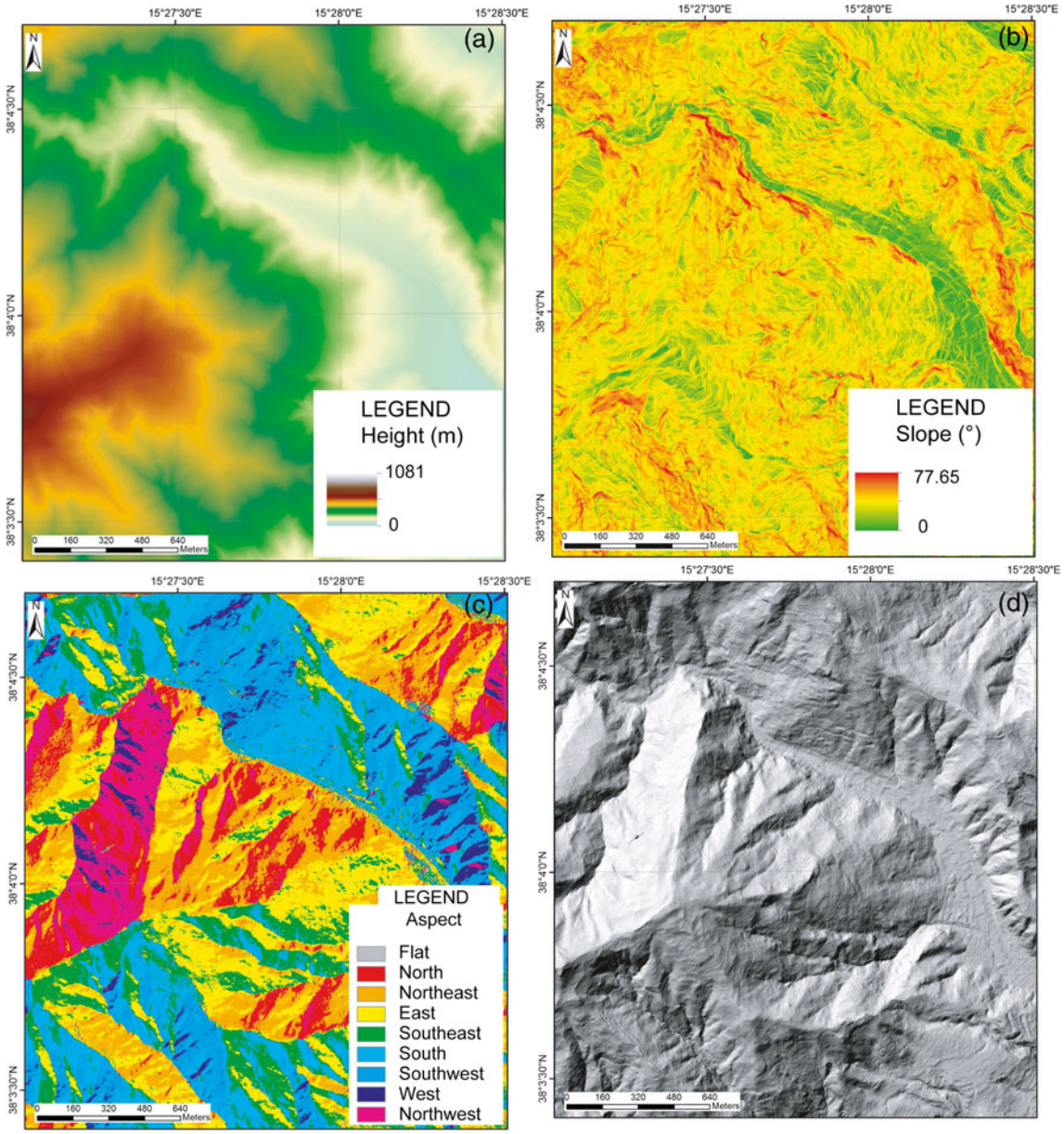

Fig. 4 Example of the 2-m resolution DEM-derived products for the area of Giampilieri. **a** DEM, **b** slope, **c** aspect, and **d** hillshade

Methodology

In the last decades, different SAR satellite missions have been used to study ground deformation phenomena, providing the possibility to reconstruct the past deformation of the areas of interest. The European C-band missions ERS 1/2, environmental satellite (ENVISAT), routinely acquired images between 1992 and 2010. These data can be coupled with the currently operating C-band sensors, such as RADARSAT 1/2 and X-band sensors (TerraSAR-X and COSMO-SkyMed (constellation of small satellites for the Mediterranean basin Observation)), allowing the analysis of both past and recent ground displacements of the observed scenes, in a time interval of more than 20 years (Bianchini et al. 2013). PSInSAR (and its evolution SqueeSAR) provides deformation time series on grids of stable reflective point-wise targets called PS or diffuse scatterers (DS), which correspond to hand-made artifacts, such as buildings, railways or highways, and/or to natural targets (rocky outcrops), characterized by a coherent electromagnetic behavior in time (Ferretti et al. 2001; 2011). The displacements recorded for each PS or DS are measured considering a stable ground point (reference point) of known coordinates. A ground deformation multi-temporal analysis can use different sensors acquiring in different periods. This means that ground deformation velocity of each PS dataset is measured along a different LOS. In order to compare different sensors data, characterized by different look angles and wavelengths, and thus different LOS, Notti et al. (2014) suggested to project the velocity, measured along the LOS, along the steepest slope (Eq. 1).

$$V_{\text{Slope}} = V_{\text{Los}}/C \tag{1}$$

Table 1 Characteristic of the used PSInSAR datasets

Area	Sensor	Geometry	Time interval	No. images	Density (PS/km^2)	Resolution (m)
San Fratello	CSK	Descending	16/01/2011–02/05/2012	32	400.62	3
Giampilieri	ENVISAT	Ascending	22/01/2003–20/05/2009	55	414.88	30

where V_{Slope} is the velocity projected along the steepest slope, V_{Los} represents the velocity measured along the satellite LOS, and C is the coefficient calculated as follows (Eq. 2):

$$C = (\text{nlos COS}(S)\ \text{SIN}(A-1.571)) + (\text{elos}\ (-1\ \text{COS}(S)\ \text{COS}(A-1.571)) + (\text{hlos SIN}(S))) \quad (2)$$

where S is the Slope, A is the Aspect both derived from the DEM and nlos, and hlos and elos are the direction cosines of the satellite LOS.

The proposed formula uses DEM-derived products such as Slope and Aspect, therefore this procedure obviously needs a DEM. Three DEMs having different resolutions (Table 1) were used to project the PS velocities along the steepest slope. The first one is the 20-m resolution DEM, created in 2002 by Italian Military Geographic Institute (IGM) and derived from the interpolation of the contour lines and the geodetic points of the, which covers the whole Sicily area. For the San Fratello landslide area, a high-resolution airborne laser scanning (ALS) DEM, acquired soon after the 2010 event, was used. This DEM is characterized by spatial resolution of 2 m and 4 p/m^2. Even for the Giampilieri area, an ALS DEM, acquired during 2009, was used to produce a 1-m resolution DEM with 8 p/m^2.

PS heights included in the PS datasets have been retrieved using the shuttle radar topography mission (SRTM) DEM (WGS84) calibrated on the basis of the reference point which usually has an accurate GPS position. The orthometric height of each PS has been deduced subtracting a correction factor (around 43 m) which considers the ellipsoid height from the SRTM height. In order to evaluate the effectiveness of the DEM resolution, first of all, the height above the sea level of each PS, retrieved by the PS dataset, was compared to the height extracted from each available DEM by using a linear regression (Fig. 5). The extraction of the PS heights from each available DEM was performed considering the height of each PS data center in GIS environment.

The second step regards the projected velocities and their directions with respect to the North and to the slope morphology (Fig. 5). In particular, the projected velocities direction was evaluated with respect to the slope orientation (Aspect). When a low-resolution DEM is used, geometrical problems can be detected especially in correspondence with watershed divides, where several velocity vectors should be oriented upslope. A visual inspection was used to detect the area affected by geometrical problems. In order to evaluate the effectiveness of different DEM resolution in PSInSAR post processing analysis, phase 2 PS dataset was used, one for each investigated area. In the San Fratello landslide area, PS data acquired with COSMO-SkyMed sensor were used to evaluate the post event ground deformation (Table 2). ENVISAT data were used to assess the pre-event deformation phenomena in correspondence of the area of Giampilieri (Table 1).

Results and discussion

The San Fratello landslide

In the San Fratello area, the results obtained by using the 20- and 2-m resolution DEMs were compared. The test site location is very useful because of its position, located across a divide between two

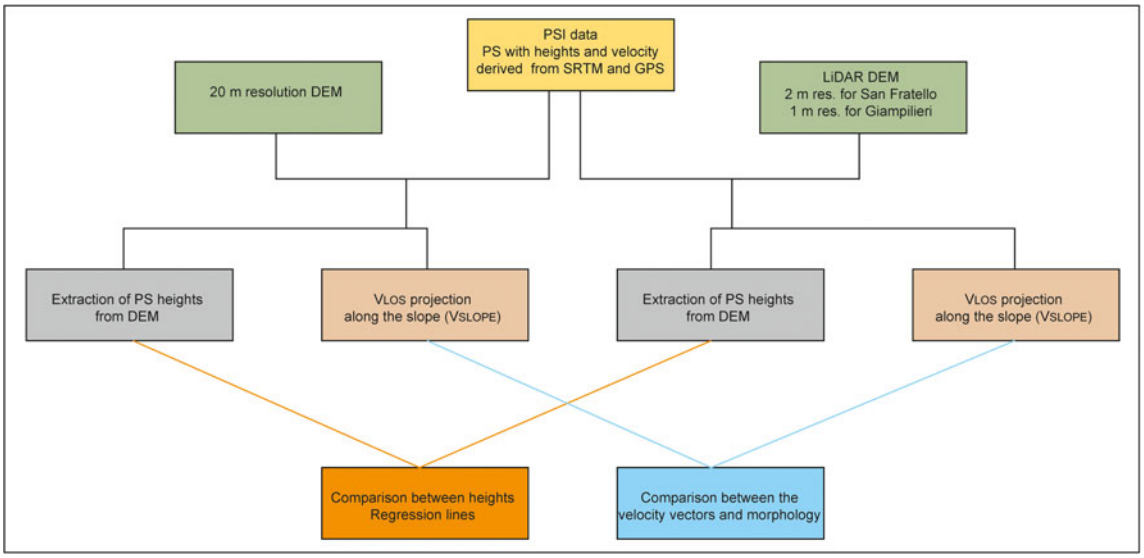

Fig. 5 Flow chart illustrating the adopted methodology

Table 2 Characteristic of the used DEMs

Area	Type	Date	Resolution
Sicily	Interpolation	2002	20 m
San Fratello	LIDAR	2010	2 m–4 p/m^2
Giampilieri	LIDAR	2009	1 m–8 p/m^2

watersheds. Along the divide, the higher the approximation introduced by a low-resolution DEM, the lower the accuracy in obtaining an accurate divide position. An example of the DEM-derived products is reported in Figs. 2 and 3. After a simple visual comparison, the 2-m resolution DEM (Fig. 3) can be considered more useful to characterize the slope morphology. In particular, both the derived Slope and hillshade clearly show several elements on the eastern slope of San Fratello such as the presence of a channel network, counterslopes, and secondary scarps that cannot be detected by using the 20-m resolution DEM (Fig. 2). Furthermore, the comparison between the two obtained Aspects highlights the presence of an area, about 200 m^2 in extension, located across the divide showing different orientation (Fig. 2c). In the 20-m resolution-derived Aspect, the N-S-oriented divide does not perfectly separate the eastward-oriented slope from the westward-oriented ones. A strip located eastward of the divide shows a westward orientation which does not correspond to the real slope morphology (Fig. 2c). This area can affect a proper projection of the ground deformation velocities along the steepest slope. Among the data included in each PS dataset (e.g., deformation, velocity), the elevation of each PS is reported. These elevations were compared to those derived by both the available DEMs in order to compare their correlations (Fig. 6). The comparison between PS elevations and those retrieved from the 20-m resolution DEM shows that the correlation between elevations is characterized by an R^2=0.59. This correlation is based on 4098 PS. A strong improvement in the correlations between the elevations was observed comparing the PS heights to the elevations extracted from the 2-m resolution DEM (Fig. 7). In this case, the R^2 is 0.99 suggesting that this DEM is strongly reliable. This correlation is also based on the same 4098 PS. Following the equation proposed by Notti et al. (2014). the PS velocities were projected along the steepest slope using both the 2- and 20-m resolution DEMs. Usually, the directions of the projected PS velocity, by using both DEMs, are in agreement with the average slope direction, except for the area characterized by a higher terrain roughness, where the 2-m resolution DEM resulted more accurate. This agreement strongly decreases in correspondence with the divide, especially in the previously mentioned area where the aspect derived from the 20-m resolution DEM shows a different orientation with respect to the real morphology. In this area, the PS velocities projected using the 20-m resolution DEM are directed upward (Fig. 8a), which is a very unlikely condition. On the contrary, projected PS velocities obtained by using the 2-m resolution DEM are in agreement with the main slope direction (Fig. 8b). Considering the unreliable projected PS velocities, it is possible to detect the area where the 20-m resolution DEM is affected by geometric problems (Fig. 8c), probably related to the approximation due to its lower resolution which increased nearby to the divide. This area includes also part of the 2010 San Fratello landslide crown. The total amount of PS located in this area is 1609 (39.26 % of the available PS) which must not be considered for a correct ground deformation analysis using the projected PS velocities. A subset of the whole PS population was extracted considering those PS located inside the detected area in order to investigate the relationship between PS elevations and DEMs elevations. A decrease of the correlation can be observed both for the 20- and 2-m resolution DEM but, while this decrease is still acceptable (R^2=0.86) for the 2-m DEM (Fig. 7a), for the 20-m DEM, it is very high (R^2=0.03) (Fig. 9b). These correlations have been assessed using a total of 1609 PS.

The Giampilieri area

The same approach described for the San Fratello site was also applied in the area of Giampilieri, in order to evaluate the differences between the 20-m resolution DEM and the available 1-m resolution DEM. In this case, PS data show a local lower density because they were elaborated by using the C-band sensor ENVISAT, which is characterized by lower spatial and temporal resolution with respect to the X-band sensor COSMO-SkyMed. The comparison among the PS heights and the elevations measured with the available DEM show a good correlation for both the 20-m and the 1-m resolution DEMs ,but, also in this case, the DEM having the higher resolution shows a better R^2=0.9992, whereas R^2 for

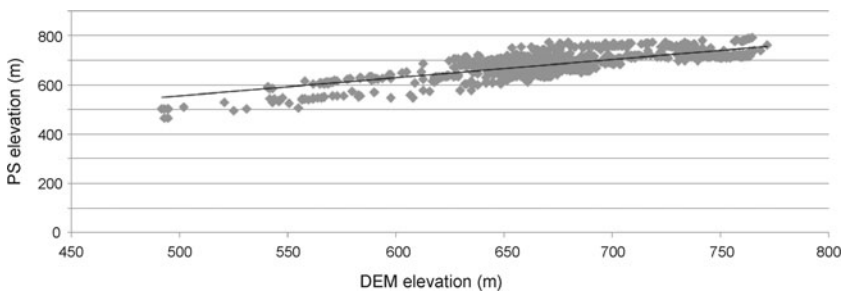

Fig. 6 Correlation between PS heights and 20-m resolution DEM elevations in the San Fratello area

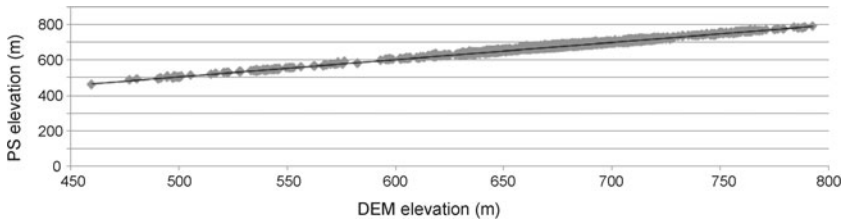

Fig. 7 Correlation between PS heights and 2-m resolution DEM elevations in the San Fratello area

the 20-m resolution DEM is equal to 0.9471 (Fig. 10). Even though also the 20-m resolution DEM shows a very good agreement between the PS heights and the related DEM elevations, when PS velocities were projected along the steepest slope direction, several geometric problems can be detected within the study area (Fig. 11). For example, north of the village of Giampilieri, several projected PS velocities, using the 20-m resolution DEM, are directed upslope (Fig. 11a);on the contrary, all the projected PS velocities using the 1-m resolution DEM are correctly oriented along the slope direction (Fig. 11b). The usefulness of the high-resolution DEM (1 m in this case) for the PS velocities projection can be appreciated especially for the areas characterized by complex relief. For example, in case of mountainous areas with narrow valleys and high difference in altitudes between the valley bottom and the divides, the higher is the DEM resolution, the more accurate will be the V_{slope} direction (see Fig. 11c, d, where most of the PS velocities projected using the 20-m resolution DEM show a very different direction with respect to those of the real morphology).

Conclusion

In this work, the reliability of high spatial resolution DEMs was tested in order to provide new opportunities and challenges for mapping landslide morphology with high accuracy, both through visual interpretation and statistical analysis.

In particular, the effectiveness of two DEMs, characterized by different resolutions, was discussed in landslide study as tools for an accurate PSInSAR post processing analysis. The comparison was made considering a high-resolution LiDAR DEM and a low-resolution DEM derived from the interpolation of contour lines. The test was performed in two different sites. For each test site, a LiDAR DEM was available. PS data measure ground deformation velocities along the LOS of the used satellite sensor. These measures can underestimate the real velocity which usually occurs along the steepest slope. Furthermore, when PS datasets are acquired by using different sensors and in different periods on the same area, they are also acquired by different LOS. In order to compare the ground deformation velocities of different PS datasets, they must be re-projected along a common direction. The steepest

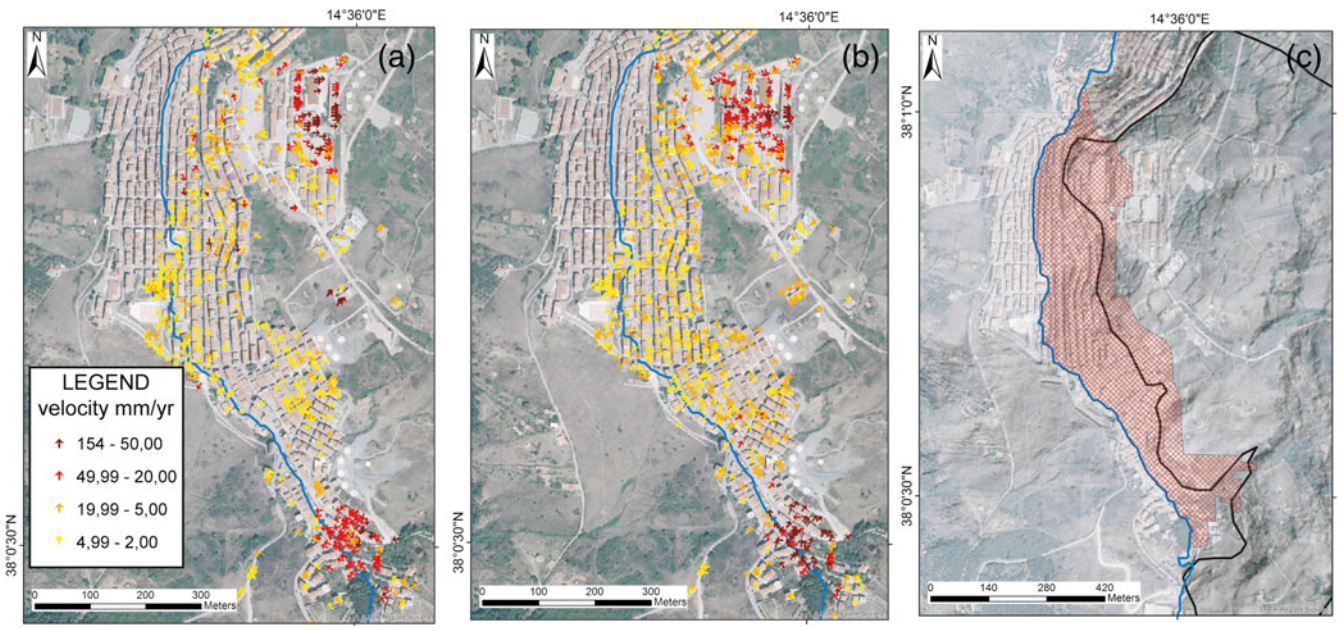

Fig. 8 Projection of the PS velocities using the 20-m resolution DEM for the crown of the San Fratello landslide (**a**) and the 2-m resolution DEM (**b**). The *blue line* represents the divide; the *black line* represents the landslide boundary. **c** delimitation of the area affected by geometrical problems

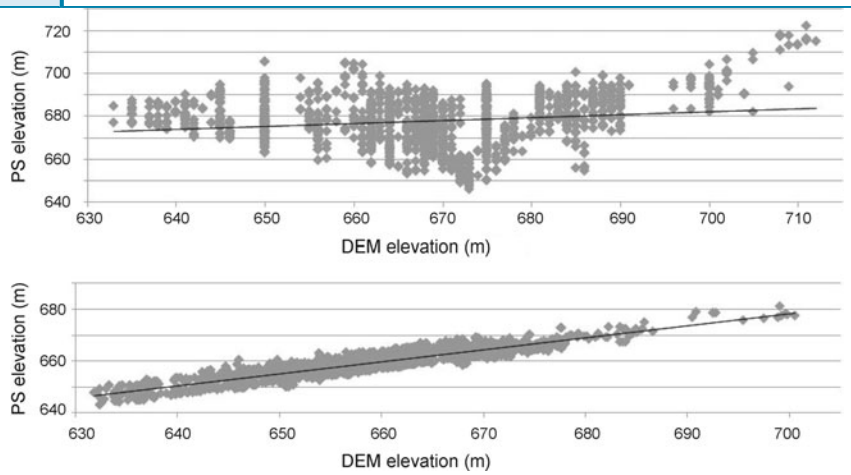

Fig. 9 Correlation between PS heights and 20-m resolution DEM elevations (**a**); correlation between PS heights and 2-m and resolution DEM elevations (**b**) for the PS located inside the area detected in Fig. 6c

slope direction is commonly considered as the most reliable and thus it can be used to project the velocities. This process needs for a DEM to calculate the characteristics of the slope where the PS are located, in particular, the formula used for the projection needs for the local value of both the slope gradient (Slope derived from a DEM) and the slope orientation (Aspect derived from a DEM).

The evaluation of the effectiveness of DEMs having different resolution in the projection of the ground deformation velocities along the steepest slope was carried out. First, by comparing the height of all the available PS with the relative DEM elevation for both the 20- and 2-m resolution DEM. Second, the velocities were projected along the steepest slope by using again both of the DEMs and identifying the presence of areas where the projected velocities show an unreliable direction (upslope). This problem particularly affects those PS located in the upper part of the slope, close to the divide, where the approximation that characterizes the low-resolution DEM does not allow a proper projection of the PS velocities along the steepest slope.

Despite the used DEMs were created in different time periods, the variation between the terrain surface heights due to possible tectonic activity is negligible. The investigated areas are tectonically active, but the vertical ground deformation measured in the long-term period highlights an overall stability during the last 15 years (Del Ventisette et al. 2013). Although the original topographic maps used to create the IGM 20-m resolution DEM can be very old (1970–1990), the height discrepancy between the latter and the ALS DEM is very high (up to 50 m) and cannot be related

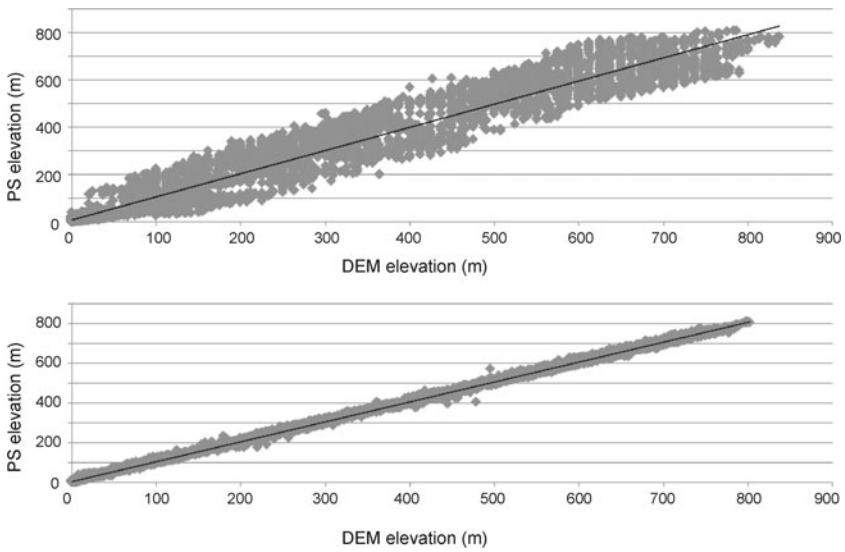

Fig. 10 Correlation between PS heights and 20-m resolution DEM elevations (**a**); correlation between PS heights and 1-m and resolution DEM elevations (**a**)

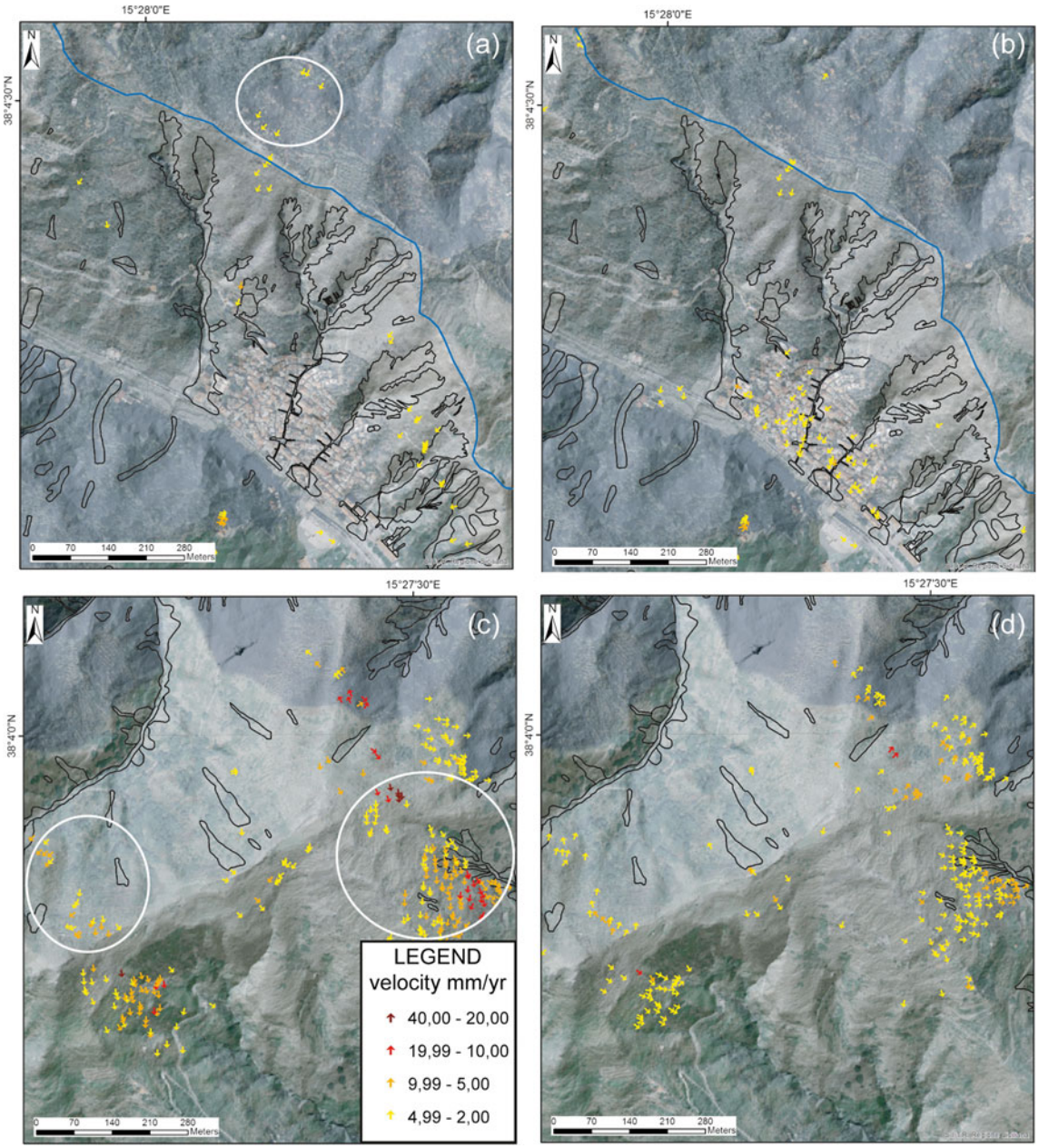

Fig. 11 **a** PS velocities projected using the 20-m resolution DEM north of the Giampilieri village (the with circle include the PS having upslope direction); **b** PS velocities projected using the 2-m resolution DEM north of the Giampilieri; **c** PS velocities projected using the 20-m resolution DEM south of the Giampilieri; **d** PS velocities projected using the 2-m resolution DEM south of the Giampilieri. The *blue line* in **a** and **b** represents the divide; the *black lines* represent the landslide boundaries of the 2009 event occurred in the area

to vertical deformation due to the tectonic activity. Considering the comparison between PS heights, derived from the SRTM data, calibrated with the reference point GPS position, and the ALS DEMs heights, a very reduced discrepancy has been recognized. This comparison can be considered as a doubleway in order to estimate the accuracy of both the data.

High-resolution topographic data have not only the potential to detect morphological characteristic (counterslopes, secondary scarps, etc.) within a landslide, but this work also highlights that a correct PSInSAR post processing analysis can benefit from the use of a high-resolution DEM, with special regards to the landslide kinematics understanding. On the contrary, the use of a medium- to low-resolution DEM can lead to geometric problems in the projection of the PS velocities, especially nearby the watershed divides and in the areas characterized by a complex morphology.

Acknowledgments

This study was funded by the Seventh Framework Programme of European Commission: Landslide Modelling and Tools for vulnerability assessment preparedness and recovery management (LAMPRE). We thank two anonymous reviewers for their suggestions which greatly improved this work. The COSMO-SkyMed data have been processed by Tele-Rilevamento Europa (TRE).

References

Ardizzone F, Cardinali M, Galli M, Guzzetti F, Reichembach P (2007) Identification and mapping of recent rainfall-induced landslides using elevation data collected by airborne lidar. Nat Hazards Earth Sist Sci 7:637–650

Ardizzone F, Basile G, Cardinali M, Casagli N, Del Conte S, Del Ventisette C, Fiorucci F, Garfagnoli F, Gigli G, Guzzetti F, Iovine G, Mondini AC, Moretti S, Panebianco M, Raspini F, Reichembach P, Rossi M, Tanteri L, Terranova O (2012) Landslide inventory map for the Briga and the Giampilieri catchments, NE Sicily, Italy. J Maps 8:176–180

Arnaud A, Adam N, Hanssen N, Inglada J, Duro J, Closa J, Eineder M (2003) ASAR ERS interferometric phase continuity. Geoscience and Remote Sensing Symposium, 2003. IGARSS Proceedings. 2003 I.E. International 1133–1135

Bardi F, Frodella W, Ciampalini A, Bianchini S, Del Ventisette C, Gigli G, Fanti R, Moretti S, Basile G, Casagli N (2014) Integration between ground based and satellite SAR data in landslide mapping: the San Fratello case study. Geophys J Roy Astron Soc 223:45–60

Berardino P, Fornaro G, Lanari R, Sansosti E (2002) A new algorithm for surface deformation monitoring based on small baseline differential SAR interferograms. IEEE Transaction on Geoscience and Remote Sensing 40:2375–2383

Bianchini S, Herrera G, Mateos RM, Notti D, Garcia I, Mora O, Moretti S (2013) Landslide activity maps generation by means of persistent scatterer interferometry. Remote Sensing 5:6198–6222

Bianchini S, Ciampalini A, Raspini F, Bardi F, Di Traglia F, Moretti S, Casagli N (2014) Multi-temporal evaluation of landslide movements and impacts on buildings in San Fratello (Italy) by means of C-band and X-band PSI data. Pure Appl Geophys. doi:10.1007/s00024-014-0839-2

Billi A, Funiciello R, Minelli L, Faccenna C, Neri G, Orecchio B, Presti D (2008) On the cause of the 1908 Messina tsunami, southern Italy. Geophysical Research Letters 35, DOI: 10.1029/2008GL033251

Bovenga F, Nutricato R, Refice A, Wasowski J (2006) Application of multi-temporal differential interferometry to slope instability detection in urban/peri-urban areas. Eng Geol 3–4:218–239

Cascini L, Fornaro G, Peduto D (2009) Analysis at medium scale of low-resolution DInSAR data in slow-moving landslide-affected areas. ISPRS J Photogram Rem Sens 64:598–611

Catani F, Lagomarsino D, Segoni S, Tofani V (2013) Landslide susceptibility estimation by random forests technique: sensitivity and scaling issues. Natural Hazards and Earth System Sciences 13:2815–2831

Cavalli M, Tarolli P, Marchi L, Dalla Fontana G (2008) The effectiveness of airborne LiDAR data in the recognition of channel-bed morphology. Catena 73:249–260

Chen Q, Liu X, Liu C, Ji R (2013) Impact analysis of differential spatial resolution DEM on object-oriented landslide extraction from high resolution remote sensing images. Ninth International on Natural Computation (ICNC), 23–25 July 2013, Shenyang, China. DOI: 10.1109/ICNC.2013.6818111

Ciampalini A, Cigna F, Del Ventisette C, Moretti S, Liguori V, Casagli N (2012) Integrated geomorphological mapping in the north-western sector of Agrigento (Italy). J Maps 8:136–145

Ciampalini A, Bardi F, Bianchini S, Frodella W, Del Ventisette C, Moretti S, Casagli N (2014) Analysis of building deformation in landslide area using multisensor PSInSARTM technique. Int J of App Earth Observ Geoinf 33:166–180

Ciampalini A, Raspini F, Bianchini S, Frodella W, Bardi F, Lagomarsino D, Di Traglia F, Moretti S, Proietti C, Pagliara P, Onori R, Corazza A, Duro A, Basile G, Casagli N (2015) Remote sensing as tool for development of landslide databases: the case of the Messina Province (Italy) geodatabase. Geomorphology. doi:10.1016/j.geomorph.2015.01.029

Cigna F, Bianchini S, Casagli N (2012) How to assess landslide activity and intensity with persistent scatterer interferometry (PSI): the PSI-based matrix approach. Landslide 10:267–283

Classens L, Heuvelink GBM, Schoorl JM, Veldkamp A (2005) DEM resolution effects on shallow landslide hazard and soil redistribution modeling. Earth Surf Process Landf 30:461–477

Colesanti C, Wasowski J (2006) Investigating landslides with space-borne synthetic aperture radar (SAR) interferometry. Eng Geol 3–4:173–199

Crosetto M, Monserrat O, Iglesias R, Crippa B (2010) Persistent scatterer interferometry: potential, limits and initial C- and X-band comparison. Photogramm Eng Remote Sens 76:1061–1069

Csatho B, Schenk T, Kyle P, Wilsond T, Krabille WB (2008) Airborne laser swath mapping of the summit of Erebus volcano, Antarctica: applications to geological mapping of a volcano. J Volcanol Geoth Res 177:531–548

Cunningham D, Grebby S, Tansey K, Gosar A, Kastelic V (2006) Application of airborne lidar to mapping seismogenetic faults in forested mountainous terrain, southeastern Alps, Slovenia. Geophys Res Lett 33:L20308

Davila N, Capra L, Gavilanes Ruiz JC, Varley N, Norini G, Vazquez AG (2007) Recent lahars at Volcán de Colima (Mexico): drainage variation and spectral classification. J Volcanol Geotherm Res 165:127–141

Del Ventisette C, Garfagnoli F, Ciampalini A, Battistini A, Gigli G, Moretti S, Casagli N (2012) An integrated approach to the study of catastrophic debris-flow: geological hazard and human influence. Nat Hazards Earth Syst Sci 12:2907–2922

Del Ventisette C, Ciampalini A, Manunta M, Calò F, Paglia L, Ardizzone F, Mondini AC, Reichembach P, Mateos RM, Bianchini S, Garcia I, Füsi B, Deak ZV, Radi K, Graniczny M, Kowalski Z, Piatkowska A, Przylucka M, Retzo H, Strozzi T, Colombo D, Mora O, Sanches F, Herrera G, Moretti S, Casagli N, Guzzetti F (2013) Exploitation of large archives of ERS and ENVISAT C-band SAR data to characterize ground deformations. Remote Sensing 5:3896–3917

Ferretti A, Prati C, Rocca F (2001) Permanent scatterers in SAR interferometry. IEEE Trans Geosci Remote Sens 39:8–20

Ferretti A, Fumagalli A, Novali F, Prati C, Rocca F, Rucci A (2011) A new algorithm for processing interferometric data-stacks: SqueeSAR. IEEE Trans Geosci Remote Sens 49:3460–3470

Frattini P, Crosta GB, Allievi J (2013) Damage to buildings in large slope rock instabilities monitored with the PSInSAR™ technique. Remote Sensing 5:4753–4773

Fuchs M, Torizin J, Kühn F (2014) The effect of DEM resolution on the computational of the factor of safety using an infinite slope model. Geophys J Roy Astron Soc 224:16–26

Gabriel AK, Goldstein RM, Zebker HA (1989) Mapping small elevation changes over large areas: differential radar interferometry. Journal of Geophysical Research: Solid Earth 94:9183–9191

Glenn NF, Streutker DR, Chadwick DJ, Thackaray GD, Dorsch SJ (2006) Analysis of LiDAR-derived topographic information for characterizing and differentiating landslide morphology and activity. Geophys J Roy Astron Soc 73:131–148

Herrera G, Davalillo JC, Mulas J, Cooksley G, Montserrat O, Pancioli V (2009) Mapping and monitoring geomorphological processes in mountainous areas using PSI data: Central Pyrenees case study. Nat Hazards Earth Syst Sci 9:1587–1598

Hung W-C, Hwang C, Chen Y-A, Chang C-P, Yen J-Y, Hooper A, Yang C-Y (2011) Surface deformation from persistent scatterers interferometry and fusion with leveling data: a case study over the Choushui River Alluvial Fan, Taiwan. Remote Sens Environ 115:957–967

Jabayedoff M, Oppikofer T, Abellán A, Derron MH, Loye A, Metzger R, Pedrazzini A (2012) Use of LIDAR in landslide investigations: a review. Nat Hazards 61:5–28

Jones AF, Brewer PA, Johnstone E, Macklin MG (2007) High resolution interpretative geomorphological mapping of river valley environments using airborne lidar data. Earth Surf Process Landf 21:1574–1592

Kasai M, Ikeda M, Asahina T, Fujisawa K (2009) LiDAR-derived DEM evaluation of deep-seated landslides in a steep and rocky region of Japan. Geophys J Roy Astron Soc 113:57–69

Keijesers JGS, Schoorl JM, Chang K-T, Chiang S-H, Claessens L, Veldkamp A (2011) Calibration and resolution effects on model performance for predicting shallow landslide locations in Taiwan. Geophys J Roy Astron Soc 133:168–177

Lagios E, Papadimitriou P, Novali F, Sakkas V, Fumagalli A, Vlachou K, Del Conte S (2012) Combined seismicity pattern analysis, DGPS and PSInSAR studies in the broader area of Cephalonia (Greece). Tectonophysics 534–525:43–58

Lagios E, Sakkas V, Novali F, Bellotti F, Ferretti A, Vlachou K, Dietrich V (2013) SqueeSAR™ and GPS ground deformation of Santorini Volcano (1992–2012): tectonic implications. Tectonophysics 594:38–59

Lavecchia G, Ferrarini F, De Nardis R, Visini F, Barbano MS (2007) Active thrusting as possible seismogenic source in Sicily (Southern Italy): some insights from integrated structural-kinematic and seismological data. Tectonophysics 445:145–167

Luo S, Fu L, Zhu S, He Q, Wan W, Yang B (2013) Processes of the displacement field change of the 2009 April 6 Mw 6.3 L'Aquila earthquake using persistent scatterer and small baseline methods. Earthquake Science 26:293–299

Marcus WA, Fonstad MA (2010) Remote sensing of rivers: the emergence of a subdiscipline in the river sciences. Earth Sur Proc Land 35:1867–1872

Massironi M, Zampieri D, Bianchi M, Schiavo A, Franceschini A (2009) Use of PSInSAR™ data to infer active tectonics: clues on the differential uplift across the Giudicarie belt (Central-Eastern Alps, Italy). Tectonophysics 476:297–303

Meisina C, Zucca F, Notti D, Colombo A, Cucchi A, Savio G, Giannico C, Bianchi M (2008) Geological interpretation of PSInsAR data at regional scale. Sensors 8:7469–7492

Meisina C, Notti D, Zucca F, Ceriani M, Colombo A, Poggi F, Roccati A, Zaccone A (2013) The use of PSInSAR™ and SqueeSAR™ techniques for updating landslide inventories. C. Margottini, P. Canuti, K. Sassa (Eds.), Landslide Science and Practice, Springer, Berlin Heidelberg, pp. 81–87

Montgomery DR, Foufoula-Georgiu E (1993) Channel network source representation using digital elevation models. Water Resour Res 29:3925–3934

Mora O, Mallorqui JJ, Broquetas A (2003) Linear and nonlinear terrain deformation maps from a reduced set of interferometric SAR images. IEEE Trans Geosci Remote Sens 41:2243–2253

Nigro F, Sulli A (1995) Plio-Pleistocene extensional tectonics in the Western Peloritani area and its offshore (northeastern Sicily). Tectonophysics 252:295–305

Notti D, Davalillo JC, Herrera G, Mora O (2010) Assessment of the performance of X-band satellite radar data for landslide mapping and monitoring: upper Tena Valley case study. Nat Hazards Earth Sist Sci 10:1865–1875

Notti D, Herrera G, Bianchini S, Meisina C, Davalillo JC, Zucca F (2014) A methodology for improving landslide PSI analysis. Int J Remote Sens 35:2186–2214

Oliveira SC, Zêzere JL, Catalão J, Nico G (2014) The contribution of PSInSAR interferometry to landslide hazard weak rock-dominated areas. Landslides 12:703–719

Oskin ME, Le K, Strane MD (2007) Quantifying fault-zone activity in arid environments with high-resolution topography. Geophys Res Lett 34:L23S05

Peltier A, Bianchi M, Kaminski E, Komorowsky J-C, Rucci A, Staudacher T (2010) PSInSAR as a new tool to monitor pre-eruptive volcano ground deformation: validation using GPS measurement on Piton de la Fournaise. Geophys Res Lett 37, L12301

Raspini F, Cigna F, Moretti S (2012) Multi-temporal mapping of land subsidence at basin scale exploiting persistent scatterer interferometry: case study of Gioia Tauro plain (Italy). J Maps 8:514–524

Rosi A, Agostini A, Tofani V, Casagli N (2014) A procedure to map subsidence at the regional scale using the persistent scatterer interferometry (PSI) technique. Remote Sensing 6:10510–10522

Tarolli P (2014) High-resolution topography for understanding Earth surface processes: opportunities and challenges. Geophys J Roy Astron Soc 216:295–312

Tarolli P, Dalla Fontana G (2009) Hillslope to valley transition morphology: new opportunities from high resolution DTMs. Geophys J Roy Astron Soc 113:47–56

Tofani V, Raspini F, Catani F, Casagli S (2013) Persistent scatterer interferometry (PSI) technique for landslide characterization and monitoring. Remote Sensing 5:1045–1065

Tomás R, Márquez Y, Lopez-Sanchez JM, Delgado J, Blanco P, Mallorquí JJ, Martínez M, Herrera G, Mulas J (2005) Mapping ground subsidence induced by aquifer overexploitation using advanced differential SAR inteferometry: Vega Media of the Segura River (SE Spain) case study. Remote Sens Environ 98:269–283

Uzielli M, Catani F, Tofani V, Casagli N (2015) Risk analysis for the Ancona landslide-I: characterization of landslide kinematics. Landslides 12:69–82

Varnes DJ (1978) Slope movements and types and processes. Landslides Analysis and Control, Transportation Research Board Special Report 176:11–33

Vilardo G, Ventura G, Terranova C, Matano F, Nardò S (2009) Ground deformation due to tectonic, hydrothermal, gravity, hydrogeological, and anthropic processes in the Campania Region (Southern Italy) from permanent scatterers synthetic aperture radar interferometry. Remote Sens Environ 113:197–212

Wasowski J, Bovenga F (2014) Investigating landslides and unstable slopes with satellite multi temporal interferometry: current issues and future perspectives. Eng Geol 174:103–138

A. Ciampalini (✉) · F. Raspini · W. Frodella · F. Bardi · S. Bianchini · S. Moretti
Department of Earth Sciences,
University of Firenze,
via La Pira, 4, 50121, Florence, Italy
e-mail: andrea.ciampalini@unifi.it